JETIR.ORG ISSN: 2349-5162 | ESTD Year : 2014 | Monthly Issue
JOURNAL OF EMERGING TECHNOLOGIES AND INNOVATIVE RESEARCH (JETIR)
An International Scholarly Open Access, Peer-reviewed, Refereed Journal

ANALYSIS OF HYDRAULIC FRACTURING AND RESERVOIR GEOMECHANICS

Nikhil Chaudhari
Department of Mechanical Engineering, JSPM NTC

Kunwar Singh K. Chadha
Department of Mechanical Engineering, JSPM NTC

Abstract: This study proposes a hydraulic fracture propagation model with a mixed mode comprising opening and sliding modes to describe a complex fracture network in a naturally fractured shale gas formation. We combine the fracture propagation model with the mixed mode and the uniaxial strain model with tectonic impacts to calculate the stress distribution using geomechanical properties. A discrete fracture network is employed to realize the fracture network composed of natural and hydraulic fractures. We compare the fracture propagation behaviors of three cases representing the Barnett, Marcellus, and Eagle Ford shale gas formations. Sensitivity analysis is performed to investigate the effects of the geomechanical properties of the reservoir on the sliding mode's contribution to the mixed mode. The numerical results highlight the significance of the mixed mode for the accurate assessment of fracture propagation behaviors in shale gas formations with high brittleness.

Keyword: XFEM, GFEM, DDM, BEM, DFN, Hydraulic Fracturing, Reservoir Geomechanics

1. INTRODUCTION

Hydraulic fracturing using a horizontal well is an essential production technique in shale gas formations. Various approaches have been developed to model hydraulic fracturing phenomena to obtain an accurate estimation of shale gas production for example, extended and generalized finite elements methods (XFEM and GFEM, respectively), displacement discontinuity methods (DDM), boundary element methods (BEM), and phase-field formulations, and discrete fracture network (DFN). The propagation of a hydraulic fracture in a naturally fractured reservoir is affected by the existence of natural fractures due to the alteration of the local stress distribution and the friction coefficients on the fracture plane. The propagation yields complex fracture geometry since the hydraulic fracture evolves in a nontrivial way due to natural fractures and geomechanical characteristics of the reservoir. Several experimental studies have investigated the interaction between hydraulic and natural fractures to comprehend fracture propagation. Criteria have been proposed to assess whether a hydraulic fracture crosses a natural fracture at the intersection between hydraulic and natural fractures. Blanton suggested a fracture-crossing criterion based on the Griffith theory [34] and performed experiments with varied intersection angles and stresses in order to study the interaction between hydraulic and natural fractures. In addition, Reshow and Pollard also proposed a fracture crossing criterion according to orthogonal intersections based on linear elastic fracture mechanics; later, this criterion was extended to no orthogonal intersections. Several numerical models have been designed to describe complex fracture networks incorporating the interaction between hydraulic and natural fractures. Developed a two-dimensional XFEM model, and simulated multiple hydraulic fractures and calculated fracture width in a naturally fractured reservoir using DDM coupled with a pseudo-three-dimensional equation.

These previous studies of fracture-crossing criteria have mainly focused on mimicking the opening mode in fracture mechanics, allowing a hydraulic fracture to cross a natural fracture directly. However, the tip of a hydraulic fracture may slip along the face of a natural fracture up to the elastic region if both fractures are encountered no orthogonally. If hydraulic fracture sliding occurs, the next step of hydraulic fracturing is either its propagation into the rock matrix or its arrest within the natural fracture. In this case, not only the opening mode but also the sliding mode becomes remarkable for fracture propagation. The significance of the sliding mode in fracture propagation has been studied analytically and numerically. For instance, suggested a fracture-crossing criterion with a mixed mode, which activated both the opening and sliding modes under the assumption that the principal stresses were given.

In the fracture-crossing criterion was derived using a linear superposition of both the opening and sliding modes. This criterion was applied to the fracture interaction in the DFN. To the best of our knowledge, researches implementing the mixed mode in the DFN are rare and need further investigation to mimic fracture behaviors more realistically with reflecting various geomechanical properties. It

is essential to obtain an accurate stress distribution to estimate in situ stresses at the location of interest since the direction of fracture propagation in porous media depends on the stress distribution around a fracture tip. To evaluate the stress distribution, the critical properties are geomechanical properties such as Poisson's ratio, Young's modulus, and the ratio of tectonic strains. As geomechanical properties vary in unconventional shale reservoirs, the estimation of hydrocarbon production needs to reflect the variability of the geomechanical properties of such reservoirs. Several studies have assessed the role of the geomechanical properties in franking. For example, a uniaxial strain model with tectonic impacts was developed to calculate in situ principal stresses from geomechanical properties. Brittleness is a geomechanical component that is useful for representing the geomechanical characteristics of shale reservoirs. Introduced the brittleness index (BI), which is calculated using Poisson's ratio and Young's modulus. The BI is regarded as an efficient indicator to evaluate the fracturing potential of an oilfield. Note that the success of shale gas production with hydraulic fracturing depends on the brittleness of shale since brittle shale's with preexisting natural fractures are hydraulically fracture-prone in the opening and sliding modes.

The purpose of this study is to show the significance of the sliding mode in franking based on the mixed mode and DFN to accurately model hydraulic fracture propagation behaviors in a naturally fractured shale reservoir. In addition, various geomechanical properties are reflected to analyses and impact on the fracture interaction. We combine a fracture propagation model with the mixed mode and a uniaxial strain model with tectonic impacts to calculate the distribution of the maximum and minimum horizontal stresses using the geomechanical properties of the reservoir. DFN is employed to realize a fracture network composed of hydraulic and natural fractures. The propagation behaviors of hydraulic fractures with mixed mode are compared with those with opening mode in three major shale gas formations: Barnett, Marcellus, and Eagle Ford. Also, the results of the comparative study are analyzed based on BI values of the shale gas formations. Finally, we perform a sensitivity analysis to investigate the effects of the geomechanical properties of the reservoir on the sliding mode's contribution to the mixed mode.

1.1 Background

Advancements in horizontal well drilling and multistage hydraulic fracturing have enabled economically viable gas productions from shale formations. Predicting productions of a fractured shale reservoir is essential for field assessments and establishing an optimum development plan. In the last decade, there have been a lot of researches to predict performances of shale gas reservoirs using a numerical simulation. It incorporates geological, geomechanical, and petro physical properties and examines their effects on gas productions. Therefore, it will be more robust than analytical or empirical methods.

Numerical simulations in shale reservoirs could be categorized into two groups. One method is to use only a reservoir simulation model, and hydraulic fracture (HF) parameters such as fracture height and half-length are considered uncertain parameters. Presented a novel approach for characterization and history matching of hydrocarbon production from a hydraulic fractured shale gas. They used an assisted history matching algorithm to compare production performances with actual responses and updated HF and discrete fracture network (DFN) model parameters. Their approach could characterize fracture parameters. However, it is limited on the specific fracture design which was done already.

1.2. Propagation of Hydraulic Fracturing in a Naturally Fractured Reservoir

1.2.1 Fracture Propagation and Modes I, II, and III in Fracture Mechanics.

In past studies, fracture propagation has been analyzed based on the linear elastic fracture mechanics theory under the assumption that the material is isotropic, linear elastic, and has a quasistatic and isothermal deformation. Researchers have applied the linear elastic fracture mechanics theory to porous media. This theory is valid only if an inelastic deformable zone at a fracture tip is small compared to the fracture size. The stress field near the fracture tip can be computed using the theory of elasticity. Figure 1 illustrates three modes of fracture propagation: Mode I, Mode II, and Mode III. Mode I is the opening mode caused by tensile stress perpendicular to the fracture plane. Mode II is the sliding mode (i.e., the in-plane shear mode), which results from shear stress acting parallel to the fracture surface and perpendicular to the fracture front. Mode III is the tearing mode (i.e., the ant plane shear mode), which is induced by shear stress acting parallel to both the fracture surface and the fracture front. Fracture growth can be modelled using each mode or a combination of modes, which is referred to as a mixed mode. Mode I lead to in-plane tensile propagation. A mixed mode composed of Mode I and Mode II (i.e., in-plane shear) results in bent fractures or sharp kinks, while a mixed mode consisting of Mode I and Mode III (i.e., antiplane shear) causes segmented fracture fronts. As fracture segmentation mostly occurs in unconsolidated or less-consolidated materials, this study focuses on comparing the effects of pure Mode I and those of a mixed mode (Mode I and Mode II) on hydraulic fracture propagation in a naturally fractured shale reservoir.

1.2.2. Fracture Crossing between Hydraulic and Natural Fractures

The presence of natural fractures in a shale reservoir affects the propagation of hydraulic fractures, thereby leading to the generation of a complex fracture network. There are four interaction types when a hydraulic fracture encounters a natural fracture, as shown in Figure 2. First, a hydraulic fracture can directly cross a natural fracture without changing its original propagation direction (Figure 2(a)). Second, a hydraulic fracture can join a natural fracture and create a new fracturing path at the tip of the natural fracture (Figure 2(b)). Third, a hydraulic fracture can be diverted along a natural fracture and kink out at a weak point of the natural fracture (Figure 2(c)). Last, a hydraulic fracture Geofluids

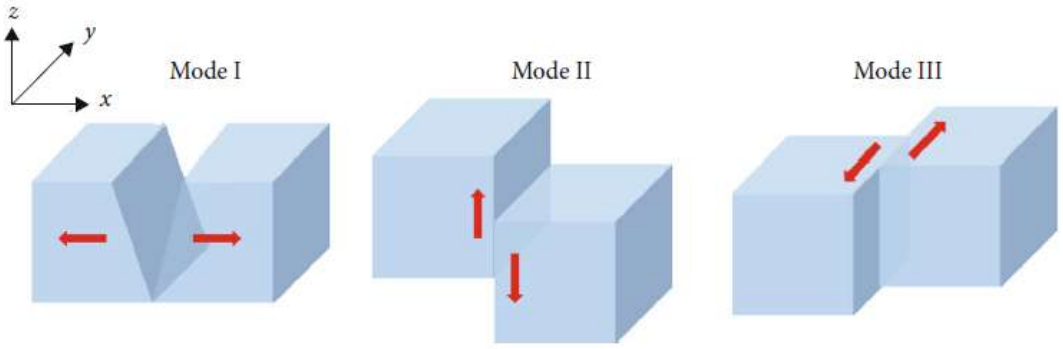

Figure 1.1: Three modes of fracture propagation: Mode I (opening mode), Mode II (sliding mode), and Mode III (tearing mode).

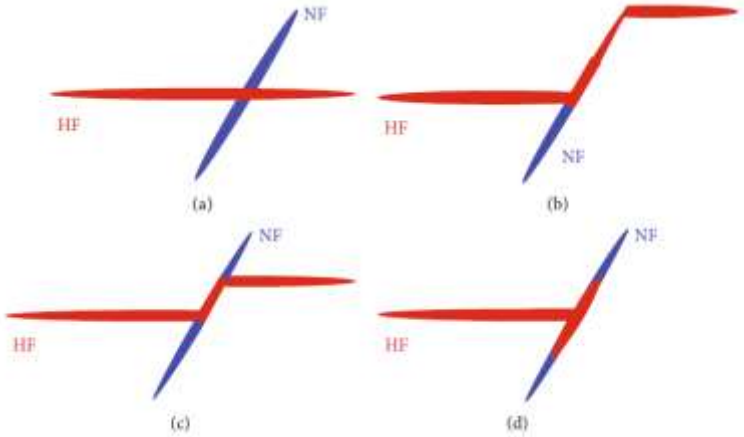

Figure 1.2: Four interaction types between a hydraulic fracture (HF) and a natural fracture (NF). (a) Direct cross. (b) Cross at a natural fracture tip. (c) Cross with an offset. (d) Arrest.

Can be arrested within a natural fracture (Figure 2(d)). For a hydraulic fracture to cross a natural fracture, two conditions must be satisfied. When the maximum principal stress reaches the tensile strength of porous media, a new fracture is initiated on the opposite side of the natural fracture interface. Also, there should be no shear slippage in the face of the natural fracture. Properties of a material interface, such as frictional resistance and cohesion, control the material's critical point to prevent slipping or allow fracture crossing.

2. MATERIALS AND METHODS

2.1. Diagnostic Fracture Injection Test.

The diagnostic fracture injection test is useful to infer geomechanical properties including fracture closure stress, reservoir pressure, leadoff coefficient, and permeability. A small volume of fluid is injected into the formation, and it creates a hydraulic fracture. After the injection, the pressures in the wellbore are monitored for several days and these data are analyzed using special plots. A typical DFIT sequence is shown in Figure 1. The analysis of DFIT data is conducted in two ways: before-closure analysis and after-closure analysis. Before closure analysis focuses on the early pressure falloff period and provides fracture closure stress, instantaneous shut-in pressure (ISIP), and leak off mechanism and coefficient. When the surface injection is stopped, the friction decreases rapidly and ISIP could be derived which is the sum of closure stress and net pressure. ISIP is estimated by placing a straight line on the pressure falloff plot. Suggested a *G*-function, which is a dimensionless measure of time to investigate the pressure decline behavior (as shown in the equations below).

$$\Delta t_D = \frac{t - t_p}{t_p}, \ldots\ldots\ldots\ldots\ldots\ldots\ldots\ldots\ldots\ldots\ldots\ldots (1)$$

$$g(\Delta t_D) = \frac{4}{3}[(1 + \Delta t_D)^{1.5} - (\Delta t_D)^{1.5}] \ldots\ldots\ldots\ldots\ldots\ldots\ldots\ldots\ldots\ldots\ldots\ldots (2)$$

$$G(\Delta t_D) = \frac{4}{\pi}[g(\Delta t_D) - g_0] \ldots\ldots\ldots\ldots\ldots\ldots\ldots\ldots\ldots\ldots\ldots\ldots (3)$$

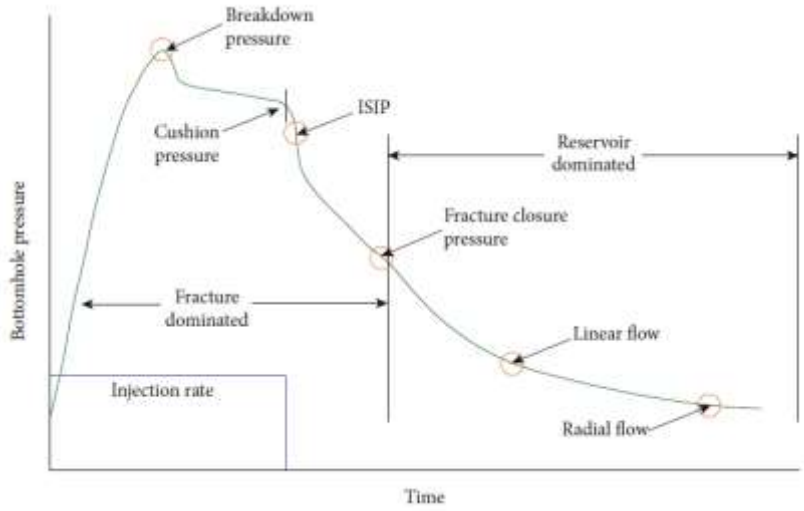

Figure 2.1: DFIT pressure response.

Where *t*p is the pumping time, *t* is the actual time, Δ*t*D is the dimensionless shut-in time, *g* is the average decline rate function, *g*0 is the initial decline rate, and *G* is the dimensionless pressure difference function.

According to the leak off mechanisms, pressure derivative (dp/dG) and *G*-function derivative (Gdp/dG) curves show characteristic shapes (Figure 2). In the normal leak off, the fracture surface area for leaking fluid is constant so the *G*-function derivative curve is a straight line before closure. The fracture closure is identified when the *G*-function derivative starts to deviate downward from the straight line. The pressure-dependent leak off (PDL) indicates the existence of natural fracture and shows a "hump" trend in the *G*-function derivative. The leak off rate of the fracture height recession or transverse storage is relatively smaller than the normal leak off, and it has a "belly" trend below the linearity of the *G*-function derivative. Fracture tip extension means that a fracture continues propagating after the shut-in caused by ultralow permeability of the formation.

3. MODELING OF HYDRAULIC FRACTURE PROPAGATION

Section 3 describes the workflow of this study for fracture propagation modeling. We combined a previous model [44] and a uniaxial strain model with tectonic stress [49]. By assuming that the overburden stress is higher than the horizontal stress in the formation, this study assumes that fracture propagation occurs on the horizontal plane (i.e., the *x*-*y* plane) with a constant fracture height identical to the formation thickness. The porous medium is linearly elastic, isotropic except for principal stresses, and has a quasistatic and isothermal deformation. In reality, the growth of a fracture depends on the injection pressure or injection rate. For simplicity, a hydraulic fracture is allowed to grow up to the maximum fracture half-length set a priori with reference to [70]. In other words, the preset value is the stopping condition for numerical simulation. As this study does not solve the flow of fracturing fluid during franking, no uncertainties such as fracturing fluid leak are taken into account. Modeling fluid-flow-driven fracturing propagation in the DFN is under investigation as our future work.

3.1. Variables for the modeling of Hydraulic Fracture

Propagation Figure 3 shows a schematic of hydraulic fracture propagation crossing a natural fracture with the model variables used in this study. To create multiple transverse hydraulic fractures to enhance hydrocarbon productivity, it is preferable to drill a horizontal well parallel to the direction of the minimum horizontal stress σh [71]. In this case, induced hydraulic fractures are normal to the direction of σh, and this normal vector is identical to the direction of the maximum horizontal stress σH [8]. As shown in Figure 3, in reality, the direction of the horizontal well drilling deviates from the direction of σh due to field constraints. As a result, the fracture initiates no orthogonally from the horizontal well; in other words, the fracture propagation direction is not parallel to the direction of σH. Let α be the inclination angle between the originally intended fracture propagation direction and σH. Note that the principal horizontal stresses (σh and σH) and α are used to calculate the coupled stress field $[\sigma x, \sigma y, \tau xy]$T (Section 3.2.1).

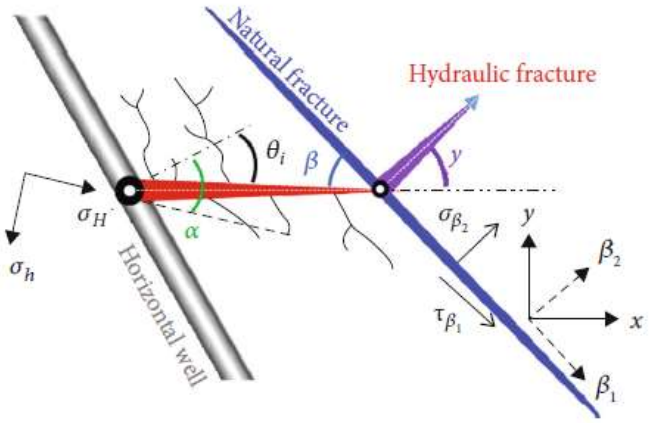

Figure 3.1: Schematic of hydraulic fracture propagation crossing a natural fracture.

The next step is to determine the fracture initiation angle θi (Section 3.2.2). If the growing hydraulic fracture meets a preexisting natural fracture, the intersection angle between the two fractures β is obtained (Section 3.2.3). Here, β is the factor that is used to determine whether either fracture crossing or sliding occurs at the intersection. If β is greater than the minimum fracture-crossing angle, fracture crossing occurs with the fracture reinitiating angle γ (Section 3.2.4). Otherwise, the hydraulic fracture slides along the natural fracture until reaching a weak point within the natural fracture at which fracture reinitiating is possible.

3.2. Workflow for the modeling of Hydraulic Fracture Propagation

The variables presented in Figure 3 are calculated according to the workflow of this study. Detailed calculations can be found in the following subsections of the present section. The first step is to stochastically generate a natural fracture network using the DFN model developed by the coordinates of natural fractures and the horizontal well are stored. Also, the maximum fracture half-length *a*max is preset. The in situ stresses are calculated. Secondly, a hydraulic fracture is initiated from a horizontal well using the fracture initiation criterion. If the hydraulic fracture encounters a natural fracture, a decision is made using the fracture crossing criterion to determine whether the hydraulic fracture crosses the natural fracture. If the cross is activated, the model calculates the fracture reinitiating angle γ and precedes the fracture propagation with this angle. Otherwise, the hydraulic fracture evolves within the natural fracture. The processes are repeated until the sum of the lengths of all connected fractures becomes greater than or equal to *a*max. Lastly, grid mapping is conducted to transfer the fracture network data of the DFN model (e.g., the coordinates of fractures and the gridlock index of a fracture network). A total connected fracture volume (TCFV) is computed from the DFN model. Oil production can be estimated if a fluid flow simulator is coupled with the DFN model through grid mapping. In this study, all source codes were written in the C programming language.

3.2.1. Estimation of In Situ Stresses

For isotropic porous media under uniaxial strain with tectonic stress effects, the minimum horizontal stress σh and the maximum horizontal stress σH are calculated using Equations (1) and (2), respectively

$$\sigma_h = \frac{v}{1-v}(\sigma_v - \delta_1\rho) + \delta_1\rho + \frac{E}{1-v^2}(\varepsilon_h + v\varepsilon_H) \dots\dots\dots\dots\dots\dots\dots\dots\dots\dots (1)$$

$$\sigma_H = \frac{v}{1-v}(\sigma_v - \delta_1\rho) + \delta_1\rho + \frac{E}{1-v^2}(\varepsilon_H + v\varepsilon_h) \dots\dots\dots\dots\dots\dots\dots\dots\dots\dots (2)$$

Where v is Poisson's ratio, σv is the vertical stress, $\delta 1$ is Biot's coefficient, p is the pore pressure, E is Young's modulus, εh is the minimum tectonic strain, and εH is the maximum tectonic strain. On the right-hand side of each equation, the sum of the first two terms corresponds to the uniaxial strain condition while the third term corresponds to the tectonic stress effects.

4. RESULTS AND DISCUSSION

In order to analyses the effects of the mixed mode on fracture propagation behaviors, we applied the developed model to fractured reservoirs mimicking the Marcellus, Barnett, and Eagle Ford shale formations. In addition, the results of the comparative study are analyzed based on the BI values of the shale gas formations.

4.1. Experimental Setting.

Figure 6 depicts a base system of DFN, and Table 3 summarizes the input data (i.e., reservoir properties and well configuration) of the base system. This system has σh in the W-E direction. A four-stage (A, B, C, and D) hydraulic fracturing was completed for a horizontal well with an α of 15°. The length of the horizontal well is 473 m, *a*max is 61 m, μ is 0.7, and $\delta 1$ is 1. Table 4 presents the geomechanical properties of the Marcellus, Barnett, and Eagle Ford shale formations. For v and *ED*, the range and the mode with the highest frequency were acquired from Yenugu , resulting in three different BI values. Since these properties are dynamic properties obtained from well logging, *ED* values were converted into E values using Equation (16). Representative values of εH and εh were obtained from Dolinar. For a hydraulic fracture to initiate on the opposite side of a natural fracture face, the maximum principal stress

must be equal to the rock's tensile strength *T*0. Here, the values of *T*0 were constants of 3, 4, and 6MPa for the Marcellus, Barnett, and Eagle Ford formations, respectively. Although this study utilises field data acquired from references (Table 4), the domain shown in Figure 6 is synthetic. For a fair comparison, all the three shale formation cases use the same domain. As a consequence, the same *a*max is given to each case.

4.2. Comparison of Fracture Propagation Behaviors in Three Shale Formations.

Using the developed model with the mixed mode, we compare fracture propagation behaviors in the three shale formations using the mode values of the geomechanical properties presented. The inclination angle α of 15° yielded a fracture initiation angle θi of 7.5°. The simulation results with the mixed mode were also

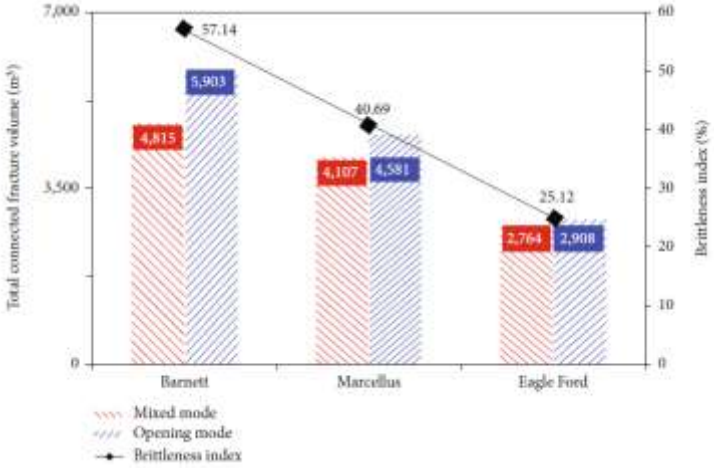

Figure 4.1: Total connected fracture volume (TCFV) obtained using mixed and opening modes.

Compared with the simulation results with the opening mode to highlight the effects of the mixed mode on fracture propagation. Figure 7 shows the simulation results for the evolved fracture networks with and without the sliding mode for the three shale formations. All shale formations were given an identical initial natural fracture network. We monitored whether the hydraulic fracture initiated from Stage A crossed the natural fracture, where their intersection is pointed out in a dashed circle in Figure 7. At the intersection in the dashed circle, β was 69°. Then, we calculated the minimum fracture-crossing angles using the inequality (7). The calculated minimum fracture-crossing angles were 58°, 73°, 85°, 53°, 65°, and 80°, respectively. Based on these results, adopting either an opening mode or a mixed mode resulted in fracture-crossing at the intersection for Marcellus and Eagle Ford cases. Interestingly, for the Barnett case with the mixed mode, the hydraulic fracture did not cross the natural fracture as β of 69° was less than the minimum fracture-crossing angle of 73°. The hydraulic fracture grew at the tip of the connected natural fracture. However, when adopting the opening mode, the hydraulic fracture crossed the natural fracture at their intersection as the minimum fracture-crossing angle decreased to 65°. This result highlights the significance of implementing the mixed mode for the accurate modeling of fracture propagation. Based on the BI values of the three shale formations, we examined the effects of fracturing modes on the TCFV. When using the mode values for v and E, the BI values were 57.14%, 40.69%, and 25.12% for the Barnett, Marcellus, and Eagle Ford formations, respectively. Here, TCFV means the total fracture volume connected to the horizontal well. Figure 8 summarizes the TCFV estimates with and without the sliding mode. The TCFV values obtained using the mixed mode were 4,815, 4,107, and 2,764m3 for the Barnett, Marcellus, and Eagle Ford

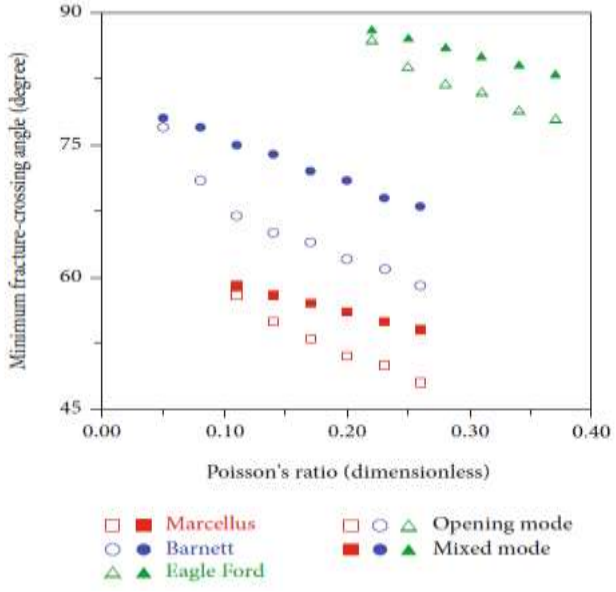

Figure 4.2: The effect of Poisson's ratio on the minimum fracture crossing angle.

Formations, respectively. For all the formations, ignoring the sliding mode led to the overestimation of the TCFV values. The TCFV values obtained using the opening modes were 5,903, 4,581, and 2,908m3 for the Barnett, Marcellus, and Eagle Ford formations, respectively. The greater the BI value was, the greater the TCFV was since fracture-crossing occurred easily. In other words, if the value of BI was relatively high such as in the Barnett shale formation, the fracture network resulted in a large deformation longitudinally rather than transversely.

4.3 Numerical methods for hydraulic fracturing modeling

Hydraulic fracturing basically involves three processes: (1) the deformation of fracture surfaces; (2) the fluid flow within the fracture; (3) the fracture propagation. Linear elasticity is usually used as the deformation law of rock; power law fluid is set for the fluid within the fracture; linear elasticity fracture mechanics theory is usually adopted as the propagation law; an additional term is often given to the fluid flow equation to calculate the leak off effects. The theoretical models of hydraulic fracturing have been developed for more than half a century. The classic hydraulic fracturing 2D models contain PKN model and KGD model. Green and Sneddon studied the problem of a flat elliptic crack under constant loading. PKN is applicable when fracture length is much larger than the height, because it assumes a plain strain in vertical direction; while KGD model assumes the crack width in horizontal is independent of its vertical position, thus, it is only reasonable when the height is much greater than its length. In order to investigate the fracture propagation with different height, Pseudo-3D (P3D) models have been developed based on PKN models. Mainly, there are two categories in P3D modes: one is cell-based models in which fracture has been divided into several self-similar cells along horizontal direction. Another is known as 'lumped model', which assumes a fracture consists of two half ellipses of equal lateral extent but different vertical extent. However, these models cannot simulate fracturing with arbitrary shape, and palaeo stress would be regionally inversed in some field, which would cause widespread horizontal micro-cracks, and excess leak off and fissure pressure storage would make pseudo- 3D models and linear-elasticity inappropriate. Thus, planar 3D (PL3D) models have been developed. In PL3D models, fracture and the coupled fluid are simulated either moving triangular mesh, or fixed rectangular mesh. PL3D assumes that the shape of hydraulic fracture is arbitrary and can be represented by a Green's function. But it requires a consistency condition between layers, and cannot simulate 'out of plane' fractures, and the use of Green's function makes it not easy for nonlinear or anisotropic rocks

Conclusions

This study analyzed the fracture propagation behaviors in shale gas reservoirs through simulations considering the effects of the mixed mode and the geomechanical properties of the reservoir mimicking three shale gas formations: Marcellus, Barnett, and Eagle Ford. The fracture propagation model was implemented with the mixed mode that linearly superimposed the opening mode and sliding mode and was combined with the uniaxial strain model. In our simulation results, the propagation results differed depending on the shale formation and fracture mode. We examined the effects of fracturing modes on the TCFV based on the BI value of each shale formation. In particular, the results indicate that neglecting the sliding mode might lead to an overestimation of the productivity in shale gas reservoirs with high BI values. In addition, the results of sensitivity analysis for various geomechanical properties revealed that the influence of the sliding mode increased when Poisson's ratio increased, strain anisotropy increased, and Young's modulus decreased. The sensitivity analysis implies that the proposed approach is extendable to other fields. In conclusion, our simulation results highlighted the significance of implementing the sliding mode in the mixed mode for the accurate modeling of fracture propagation in shale reservoirs with high brittleness.

References

[1] F. Javadpour, D. Fisher, and M. Unsworth, "Nanoscale gas flow in shale gas sediments," Journal of Canadian Petroleum Technology, vol. 46, no. 10, pp. 55–61, 2013.
[2] N. R. Warpinski, M. J. Mayerhofer, M. C. Vincent, C. L. Cipolla, and E. P. Lolon, "Stimulating unconventional reservoirs: maximizing network growth while optimizing fracture conductivity," Journal of Canadian Petroleum Technology, vol. 48, no. 10, pp. 39–51, 2013.
[3] M. Y. Soliman and C. S. Kabir, "Testing unconventional formations," Journal of Petroleum Science and Engineering, vol. 92-93, pp. 102–109, 2012.
[4] W. Yu, Z. Luo, F. Javadpour, A. Varavei, and K. Sepehrnoori, "Sensitivity analysis of hydraulic fracture geometry in shale gas reservoirs," Journal of Petroleum Science and Engineering, vol. 113, pp. 1–7, 2014.
[5] J. Kim, Y. Jang, H. Seomoon, and W. Sung, "The sorption corrected multiwall DE convolution method to identify shale gas reservoir containing sorption gas," Journal of Petroleum Science and Engineering, vol. 159, pp. 717–723, 2017.
[6] E. Gordeliy and A. Peirce, "Coupling schemes for modeling hydraulic fracture propagation using the XFEM," Computer Methods in Applied Mechanics and Engineering, vol. 253, pp. 305–322, 2013.
[7] P. Gupta and C. A. Duarte, "Simulation of non-planar three-dimensional hydraulic fracture propagation," International Journal for Numerical and Analytical Methods in Geo mechanics, vol. 38, no. 13, pp. 1397–1430, 2014.
[8] J. Kim and G. J. Moridis, "Numerical analysis of fracture propagation during hydraulic fracturing operations in shale gas systems," International Journal of Rock Mechanics and Mining Sciences, vol. 76, pp. 127–137, 2015.
[9] J. Kim, "A new numerically stable sequential algorithm for coupled finite-strain leas to plastic geomechanics and flow," Computer Methods in Applied Mechanics and Engineering, vol. 335, pp. 538–562, 2018.
[10] J. E. Olson, "Multi-fracture propagation modeling: applications to hydraulic fracturing in shales and tight gas sands," in 42nd U.S. Rock Mechanics Symposium and 2nd U.S.-Canada Rock Mechanics Symposium, San Francisco, CA, USA, 2008.

[11] V. Sesetty and A. Ghassemi, "Simulation of hydraulic fractures and their interactions with natural fractures," in 46th U.S. Rock Mechanics/Geomechanics Symposium, Chicago, IL, USA, 2012.
[12] K. Wu and J. E. Olson, "Simultaneous multi fracture treatments: fully coupled fluid flow and fracture mechanics for horizontal wells," SPE Journal, vol. 20, no. 2, pp. 337–346, 2015.
[13] X. Zhang, R. G. Jeffrey, and M. Thiercelin, "Deflection and propagation of fluid-driven fractures at frictional bedding interfaces: a numerical investigation," Journal of Structural Geology, vol. 29, no. 3, pp. 396–410, 2007.
[14] T. Xu, P. G. Ranjith, A. S. K. Au et al., "Numerical and experimental investigation of hydraulic fracturing in kaolin clay," Journal of Petroleum Science and Engineering, vol. 134, pp. 223–236, 2015.
[15] F. Paknia, A. Ghassemi, and M. PourNik, "A semi-analytical boundary element method to modeling and simulation of fluiddriven single/multi fractures in reservoirs," in SPE Liquids-Rich Basins Conference - North America, Odessa, TX, USA, 2019.
[16] M. F. Wheeler, T. Wick, and W. Wollner, "An augmented-Lagrangian method for the phase-field approach for pressurized fractures," Computer Methods in Applied Mechanics and Engineering, vol. 271, pp. 69–85, 2014.
[17] A. Mikelic, M. F. Wheeler, and T. Wick, "A phase-field method for propagating fluid-filled fractures coupled to a surrounding porous medium," Multiscale Modeling & Simulation, vol. 13, no. 1, pp. 367–398, 2015.
[18] S. Lee, M. F. Wheeler, and T. Wick, "Pressure and fluid-driven fracture propagation in porous media using an adaptive finite element phase field model," Computer Methods in Applied Mechanics and Engineering, vol. 305, pp. 111–132, 2016.
[19] T. Wick, G. Singh, and M. F. Wheeler, "Fluid-filled fracture propagation with a phase-field approach and coupling to a reservoir simulator," SPE Journal, vol. 21, no. 3, pp. 0981–0999, 2016.
[20] S. Lee, M. F. Wheeler, T. Wick, and S. Srinivasan, "Initialization of phase-field fracture propagation in porous media using probability maps of fracture networks," Mechanics Research Communications, vol. 80, pp. 16–23, 2017.